

# Effect of the addition of hydroxyl-terminated polydimethylsiloxane to TEOS-based stone protective materials

Feigao Xu · Dan Li

Received: 3 August 2012 / Accepted: 17 November 2012 / Published online: 27 November 2012  
© Springer Science+Business Media New York 2012

**Abstract** Inorganic–organic hybrid crack-free xerogels were obtained by using a surfactant *n*-octylamine as a catalyst containing tetraethoxyorthosilicate (TEOS) and hydroxyl-terminated polydimethylsiloxane as an additive. We studied the effect of gelling time and viscosity on PDMS–OH concentration. We have demonstrated that the addition of poly(dimethylsiloxane) (PDMS) to a silica oligomer associated with a neutral catalyst, in the presence of a surfactant, accelerated the gelling process; this reduction of the time needed for the product to gel in carbonate stones helped to achieve effective stone protection. It was found that PDMS–OH was chemically incorporated into the gel matrix via Si–O–Si bonds by FTIR analysis and an appreciable reduction of gel fracture for hybrids prepared from 3 % w/w of PDMS. Nitrogen adsorption–desorption isotherms of xerogels were measured, it showed the pore size of xerogels decrease with the addition of PDMS when concentration of PDMS was below 6 %, while xerogels showed pores in the macroporous range when adding 12 % w/w of PDMS. The protective performance evaluated by its ability to resist acid rain reveals that the protective effects were satisfying.

**Keywords** Stone protection · Hybrid gels · PDMS–OH · *n*-Octylamine

## 1 Introduction

For architectural and sculptural stone, the principal mechanism of chemical weathering is acidic dissolution of the carbonate stone [1, 2]. Much of the prior art with regard to protection of carbonate stone has relied on the use of film-forming sealers, including those based on drying oils, plant resins, waxes and epoxies, etc. [3–5]. Total failure of such sealer-based systems via entrapment of moisture behind the film is common, as is the embrittlement, clouding and discoloration of the films on environmental exposure to ultraviolet radiation [6, 7]. Progress in consolidation of deteriorated masonry stone with commercial formulations based on TEOS has been substantial since 1970s. These products polymerize, through a classic sol–gel process, in situ inside the pore structure of the disintegrating stone, and significantly increase the cohesion of the material [8]. A well-known drawback of these conservation products is their tendency to form brittle gels [9]. Cracking is generated by the high capillary pressures supported by the gel network during drying [10]. Mosquera et al. [11] has designed an innovative synthesis strategy in which the sol–gel transition occurs in the presence of a surfactant. Later, Mosquera's group has synthesized a new product by adding an organosiloxane, hydroxyl-terminated poly(dimethylsiloxane) (PDMS), to tetraethoxysilane (TEOS) in the presence of the surfactant, *n*-octylamine [12]. PDMS gives toughness and flexibility to the silica and useful hydrophobic properties.

In this study we use SEM, FTIR, TGA and N<sub>2</sub>-adsorption/desorption techniques to investigate how the formation of a TEOS-based consolidant is influenced by the addition of PDMS–OH when *n*-octylamine is used as catalyst. Two approaches including the hybrid gels formed on a plastic petri dishes surface (in vitro) and inside the porous network of a carbonate stone (in situ), assess the reduction achieved in percentage of gel cracking.

F. Xu (✉)  
College of Science, Nanchang University, Nanchang 330031,  
China  
e-mail: xufeigao@ncu.edu.cn

D. Li  
School of Environmental and Chemical Engineering,  
Nanchang University, Nanchang 330031, China

## 2 Experimental section

### 2.1 Materials

TEOS (analytical grade reagent, obtained from Sinopharm Chemical Reagent Corporation). PDMS–OH, viscosity  $\approx 4$  mPa s,  $M_n = 550$  was obtained from Sigma-Aldrich Co. Inc. The surfactant was *n*-octylamine (Aldrich) as polycondensation catalyst. All reagents were used as received without any further purification. The samples limestone are obtained from Nanjing Dou village. Mineralogical analysis and XRD showed that composition of the stone is composed of calcite (approximately 97 %), with trace amounts of quartz, alumina, and iron oxides. The limestone, with dimensions 5 cm  $\times$  5 cm  $\times$  1 cm, has been scraped off with a grinding machine, in order to give uniform surfaces and to reduce cutting imperfections. Then they were washed with water to remove the dust deposit and stored in desiccators at 25 °C and 50 % RH for 48 h prior to coating application.

### 2.2 Preparation of xerogels samples

The hybrid sols were magnetically stirred for 10 min at room temperature by mixing TEOS with ethanol. Then, water was added under vigorous stirring, and 0, 3, 6, 12 and 22 % (w/w) PDMS–OH was added drop by drop to the mixture under the same agitation. The magnetically stirring last to 2 min. Subsequently, the mixture was under 10 min of exposure to ultrasonic agitation. Lastly, *n*-octylamine was added to each sol under vigorous stirring for 30 min. Then, 2.0 mL of each sol was poured on a plastic petri dish ( $d = 9$  cm), restricting the height of the liquid column to 0.3 mm in order to not exceed typical values of critical thickness (i. e. the maximum film thickness of one coating before crack formation) [13], and then allowing to gel and dry until a constant weight was reached. Hybrid monolithic xerogels were obtained as the following methods [14]: sols of 10 mL were cast in weighing bottle of 2.40 cm in diameter and 3.2 cm in length. Dried xerogels were obtained by simple exposure of the sols to laboratory conditions by means of pinholes apertures in the lid until a constant weight was reached. Gelling time was determined by a simple visualization of the gel transition inside the plastic centrifuge tube in the slow drying (tubes were sealed on top by lids that were perforated extensively with a needle) at 25 °C.

### 2.3 Protection of stone samples

The hybrid sols were applied on stone samples by brushing under laboratory conditions until the surface remained wet for 1 min (two times wet on wet). Then, all samples were permitted to gel and age for 7 days at laboratory conditions.

### 2.4 Methods of characterization

Fourier Transform Infrared Spectroscopy was recorded employing a Nicolet Nexus 870 FTIR spectrometer. A small amount of hybrid xerogels samples were mixed with KBr and pressed into pellets, then scanned from 4,000 to 400  $\text{cm}^{-1}$ . The BET specific surface area of the powdered xerogels was obtained from  $\text{N}_2$  adsorption–desorption isotherm measured at 77 K in an automatic adsorption apparatus (ASAP2010; micromeritics). The pore size distributions were calculated by the BJH (Barret–Joyner–Halenda) method using the  $\text{N}_2$  desorption isotherm. Silica xerogels were also characterised in thermal behaviour using simultaneous differential thermal analysis (TA-SDT600), with a heating rate of 10 °C  $\text{min}^{-1}$  to 800 °C  $\text{min}^{-1}$  under flowing nitrogen (100 mL  $\text{min}^{-1}$ ). A palladium–gold alloy was vacuum evaporated onto the hybrid xerogel samples and treated stones. The outer surfaces of the xerogels and treated stones were then studied using a FEI Quanta 200F (Holand) scanning electron microscope at 15 kV of accelerating voltage under various magnifications. The contact angles were measured with a 5  $\mu\text{L}$  water droplet at ambient temperature with an optical contact angle meter (DSA100 of KRUSS Instruments Ltd., Germany). The reported values of contact angles were averages of five measurements made on different points of the sample surface. Calcium ions in circulated acid rain solution were determined by atomic absorption spectrophotometer (Varian AA240). The viscosity of sol was determined by NDJ-5S viscometer (Shanghai Pingxian Instruments Ltd., China). The bulk densities of the xerogels were determined using an immersion method. After weighing the xerogels samples, they were rapidly allowed to pour into a known volume of ethanol in scale capacity device and measure the volume by displacement of ethanol. The bulk density was calculated from the weight of the air-dried sample and the volume of the sample.

### 2.5 Evaluation of protection against acid rain attack

Three limestone samples were used to evaluate the protective ability of hybrid sol protective materials against acid rain attack. One sample was left untreated as blank. Another sample was treated on all faces with hybrid sol. For comparison, a further sample was treated with commercial fluoro-organosilane product (Coesol) by brush. Samples were sprayed with  $\text{H}_2\text{SO}_4$  solution circulated by a peristaltic pump as we designed before [15]. Each circulation lasted 8 h. The  $\text{H}_2\text{SO}_4$  solution used in the experiment was adjusted to pH 4.0 to simulate the acid rain. In circulation, the volumetric flow rate of solution was arranged at 6 mL  $\text{min}^{-1}$ , and the rate was fixed for all samples. The flow rate of solution upon samples is very important parameter in case of this kind of experimental studies.

The samples were placed at an angle of 45° in a wide beaker and the solution was dropped on the samples continuously. The spray bottle was always placed at a controlled distance from the sample in order to cover the entire surface of the limestone sample. The pH of the run-off was controlled using a calibrated pH meter.

## 2.6 Vapor permeability measurements

For the vapor permeability, sample blocks (5 × 5 × 1 cm) were fixed on the top of identical cylindrical PVC containers that were partially (1/2) filled with water. Then, the containers with stone lids were placed in a desiccator, kept at RH 20 % and at constant temperature of 30 ± 0.5 °C. The containers were weighted every 24 h. It was assumed that the vapor flow through the stone had reached a constant value when the difference between two consecutive daily (24 h) weight variations,  $\Delta M_{i-1}$  and  $\Delta M_i$ , was less than 5 % [16]:

$$\left| \frac{\Delta M_i - \Delta M_{i-1}}{\Delta M_i} \right| \times 100\% \leq 5\%$$

Under these conditions the residual vapor permeability was evaluated as daily weight variations in case of treated and untreated samples.

## 3 Results and discussion

### 3.1 Characterization of gels obtained in vitro

As an important parameter closely related with the consolidant penetration into the stone, viscosity of each sol prepared is determined at 25 °C. To compare the viscosity of various sols, the viscosity is immediately measured after PDMS–OH is added. The effect of the addition of PDMS–OH to the sols on the sol viscosity is shown in Fig. 1. It is observed a relatively small increase in viscosity depending on the amount of PDMS–OH. It can be seen sol viscosity gradually increases from 1.53 to 2.34 mPa s with the addition of PDMS. Thus, the ability to penetrate into stone substrates would remain practically unaffected since the viscosity of the commercial consolidant is commonly 2–3.3 mPa s [17]. Figure 2 shows gelling time change with PDMS–OH concentration. With increasing in concentrations of PDMS–OH, the gelling time decreases. This behavior can be explained because PDMS chains in the starting sol contain the most silanol terminals which must be hydrolyzed as a prior stage to the gel transition; therefore, the higher the PDMS content in the starting sol is, the more rapid the co-condensation process is [18]. One week after gelification took place, the thin films obtained on plastic petri dishes are examined. Within the series shown

in Fig. 3, a great effect of cracking reduction is observed beginning from the gel containing 3 % of PDMS–OH. Similar levels of reduction in cracking are observed with the addition of PDMS–OH. Information on gel morphology was acquired using SEM. In Fig. 4, there are many network pores which are composed of ultrafine spherical silica nanoparticles for the TEOS + 0.6 % *n*-octylamine without addition of PDMS–OH. However, when 12 % PDMS–OH is added to the TEOS + 0.6 % *n*-octylamine sol, the xerogel is a typical dense material. The reason may be that network pores were filled with PDMS chains. In addition, the rubbery elasticity of silica xerogels containing PDMS, responsible for their crack-free, was explained by Mosquera [18].

The investigation of the surface morphology reveals the presence of micron-sized protrusions when concentration of PDMS is 22 %. The micron-sized protrusions may be PDMS aggregates due to self-condensation of PDMS.

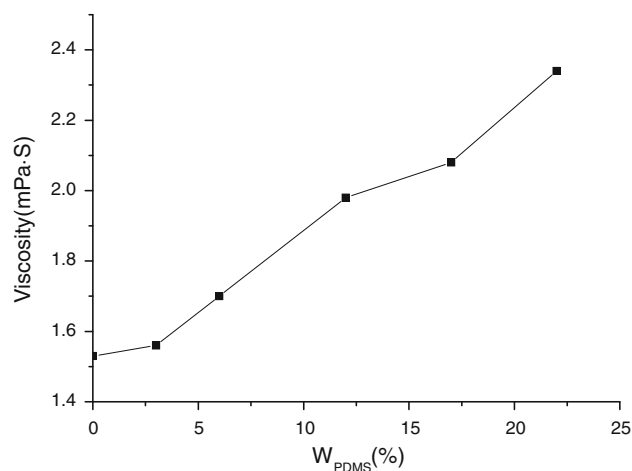


Fig. 1 The content of PDMS–OH on the viscosity (25 °C)

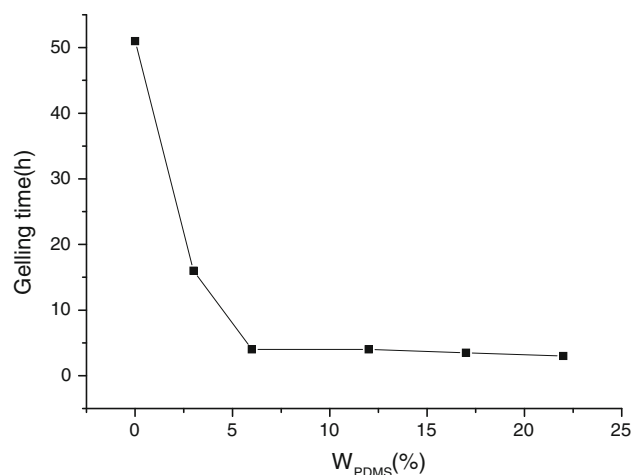
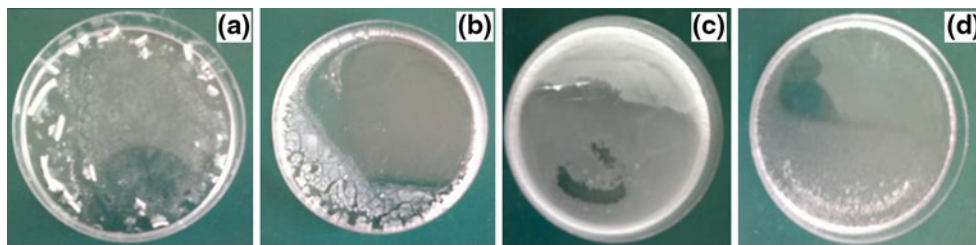
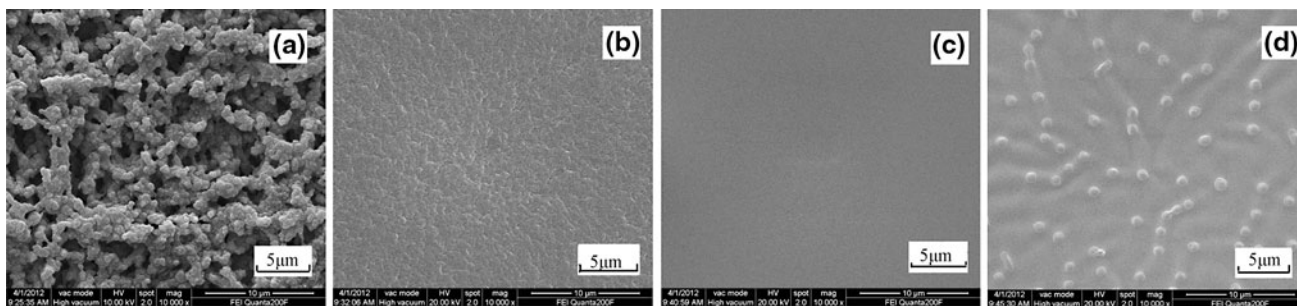


Fig. 2 The content of PDMS–OH on the gelling time (25 °C)



**Fig. 3** Photographs of hybrid gels derived from TEOS–PDMS–OH (a 0 %; b 3 %; c 12 %; d 22 %)



**Fig. 4** SEM images of four different contents of PDMS–OH (a 0 %; b 3 %; c 12 %; d 22 %)

When PDMS is mixed with TEOS, three different condensation processes may occur [19]: (1) co-condensation between two components, (2) self-condensation of PDMS, or (3) hydrolysis of TEOS and the subsequent condensation of silanols. With the addition of PDMS–OH, a part of PDMS–OH was co-condensation with TEOS, the rest of PDMS–OH was self-condensation.

FTIR transmittance spectra of the xerogels under study is shown in Fig. 5. For all TEOS/PDMS hybrid gel sample studied here, there is a very pronounced band appearing at 457, 800, 1,078  $\text{cm}^{-1}$  which corresponded to the absorption of Si–O–Si groups, indicating that hybrid gel samples

are mainly composed of a silica network [20]. The plain band centered at 3,443  $\text{cm}^{-1}$  and the sharp band at 1,637  $\text{cm}^{-1}$  are respectively assigned to the O–H stretching and bending absorptions [20]. The peak at 1,259  $\text{cm}^{-1}$  is attributed to the Si–(CH<sub>3</sub>)<sub>2</sub> bond [21, 22]. The band at 851  $\text{cm}^{-1}$  is assigned to the copolymerization reaction between Si–OH groups of hydrolyzed TEOS and Si–OH groups of PDMS molecules [21, 23]. This shows that PDMS is covalently bonded to silica particles, confirming that the copolymerization of PDMS and TEOS is effective and homogeneous organic–inorganic hybrid xerogels are created.

Hybrid xerogels are obtained derived from TEOS–PDMS–OH after drying under laboratory conditions with the addition of PDMS in Fig. 6. Within the series, a great effect of cracking reduction is observed and coloration of hybrid gels happens to change. The variations of volume shrinkage, with addition of PDMS to the sol is given in Fig. 7. The results shows that volume shrinkage and density decreases with the addition of PDMS. This could give rise to the significant increasing in the dry materials “SiO<sub>2</sub>” contents with the addition of PDMS.

Textural properties of the xerogels under study are determined from the nitrogen adsorption–desorption isotherms (Fig. 8) and are given in Table 1. The three xerogels (0, 3, 6 %) synthesized in the presence of the surfactant show type IV isotherms, which are typical of mesoporous materials, according to the IUPAC classification. Concerning the effects on textural properties for three xerogels, pore size decreases with the addition of PDMS.

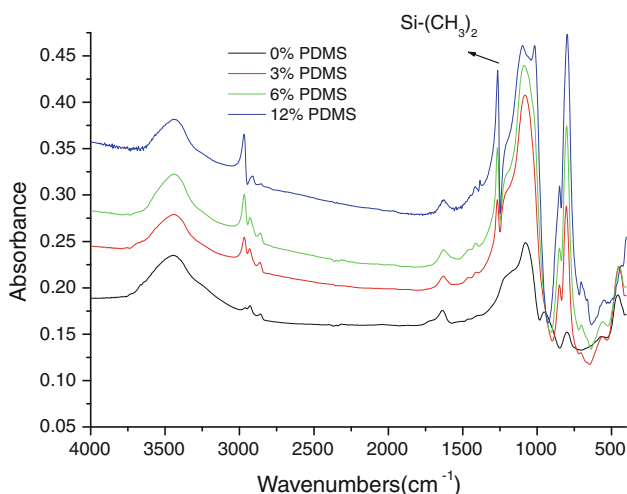


**Fig. 5** FTIR spectra of the silica xerogels under study

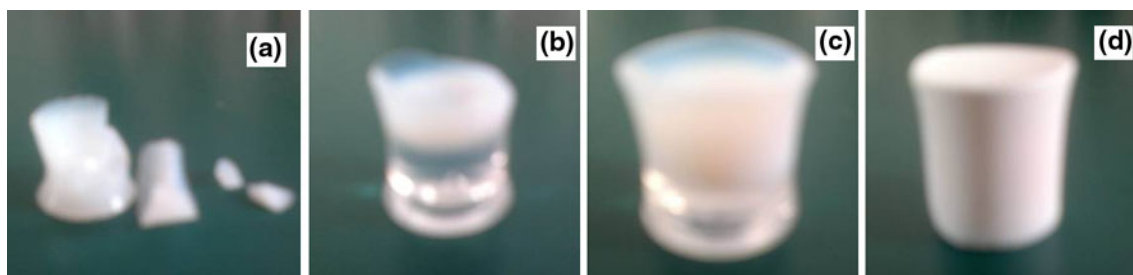


**Fig. 6** Hybrid xerogels derived from TEOS–PDMS–OH after drying under laboratory conditions (a 0 %; b 3 %; c 6 %; d 12 %)

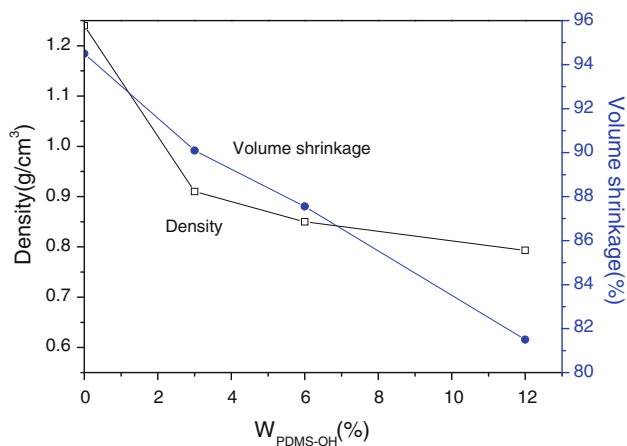


**Fig. 7** Density and volume shrinkage of dried gels with the addition of PDMS–OH (a 0 %; b 3 %; c 6 %; d 12 %)

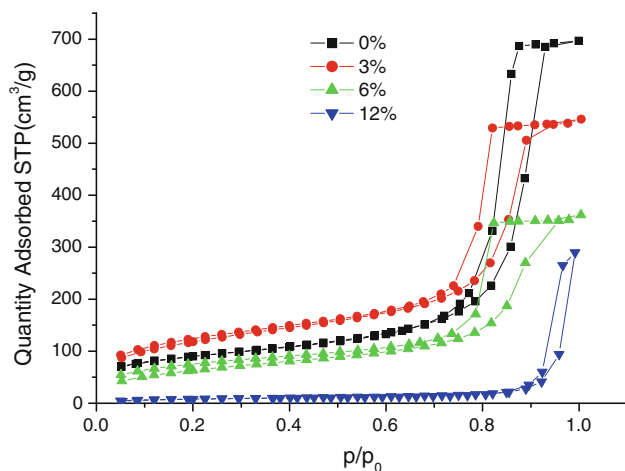


**Fig. 8** Nitrogen adsorption isotherms for the xerogels under study

Furthermore, change of pore volume is also similar. The BJH pore size distribution for the materials under study is shown in Fig. 9. The silica exhibited a narrow pore size distribution 2–25 nm. The most adsorption of xerogel (12 %) takes place at low relative pressure values, which indicates that the pore size in the network is very small, while the silica show pores in the macroporous range from BJH pore size distribution. The reason may be that with the

**Table 1** Gel properties of TEOS–PDMS–OH hybrid

| Sample        | Gel properties                                 |  |                            |
|---------------|--|--|----------------------------|
|               | Pore volume (cm <sup>3</sup> g <sup>-1</sup> ) | ABET surface (m <sup>2</sup> g <sup>-1</sup> ) | Average pore diameter (nm) |
| TEOS/0 %PDMS  | 0.49   | 321.65   | 21.2                       |
| TEOS/3 %PDMS  | 0.31   | 430.63   | 15.8                       |
| TEOS/6 %PDMS  | 0.16   | 237.30   | 15.3                       |
| TEOS/12 %PDMS | 0.33   | 34.24  | 54.7                       |

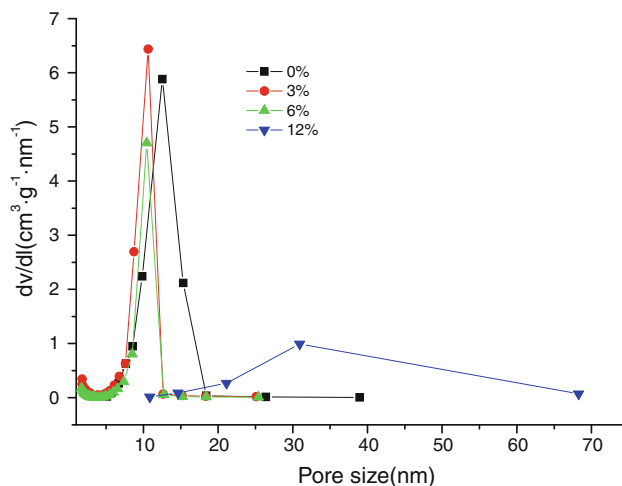
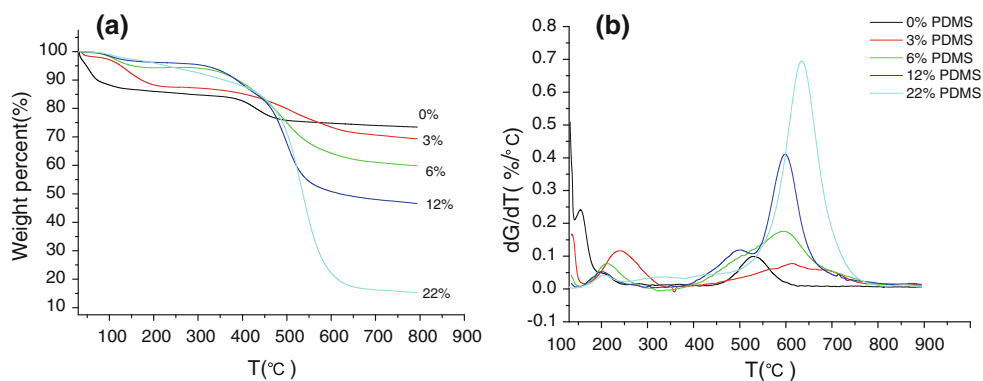


**Fig. 9** Pore size distribution for the TEOS/PDMS hybrid xerogels

addition of the PDMS, the pore size of silica becomes small, resulting in an increasing number of the interstitial holes with large size which are formed between silica particles.

TGA analysis (Fig. 10a) shows that, at 800 °C, all samples have completely lost both the water and the solvent adsorbed in the structure, as well as the un-reacted alkoxy groups, leaving behind only the total amount of SiO<sub>2</sub> formed. This concept is known as ceramic yield [24]. The xerogel synthesized without PDMS–OH presented the highest percentage of silica formed in the structure (73.5 % of ceramic yield), whereas only 15.3 % is obtained when concentration of PDMS–OH is 22 %. This is due to the

**Fig. 10** TGA analysis for hybrid xerogels **a** TGA curve, **b** derivative of TGA curve



increasing of organic groups( $\text{Si}-\text{CH}_3$ ) which are eliminated with the addition of PDMS-OH. The TGA/DTA study for 12 % PDMS is shown in Fig. 10b as an example of the thermal behavior of these types of materials. TGA derivative analysis for hybrid xerogels shows one endothermic peak (around 100 °C), which is assigned to solvent loss. A second, exothermic peak (500 °C) is assigned to the gradual disappearance of the alkyl groups. The hybrid xerogels in absence of PDMS have a much lower thermal stability as evidenced by a lower decomposing temperature at 430 °C. It is clear that the presence of the PDMS in the hybrid xerogels results in a stronger thermal stability.

### 3.2 Characterization of gels obtained in situ

The contact-angle measurement was used to evaluate the overall effectiveness of hybrid materials by considering the hydrophobicity of surfaces which is then attributed to values of contact-angle equal to or higher than 90°. Figure 11 gives the contact angle ( $\theta$ ) values for various concentration of PDMS measured using the contact angle meter. The mean  $\theta$  values were 78° for untreated limestone while  $\theta$  values of limestone treated with hybrid sol increased first and then decreased with increasing concentration of PDMS. The hybrid sol treatment induced a considerable increase of contact angle on the carbonate stone, which was attributed to methyl groups positioned along the backbone of these macromolecules [13].

A detail from the carbonate stone is presented in Fig. 12. It can be seen some aggregated carbonate stone grains as well as relatively large pores. After treating the stone with TEOS + 0.6 % *n*-octylamine led to a multi-cracked film (Fig. 12b) on the stone surface while a much more continuous and denser film was deposited when using TEOS + 0.6 % *n*-octylamine + 12 %PDMS-OH (Fig. 12c). The addition of PDMS-OH helped improve the gel resistance to fracture.

The pH variation of the run-off from the carbonate stone with time during exposure to acid rain solution of initial pH 4 is presented in Fig. 13. For untreated sample, the run-off

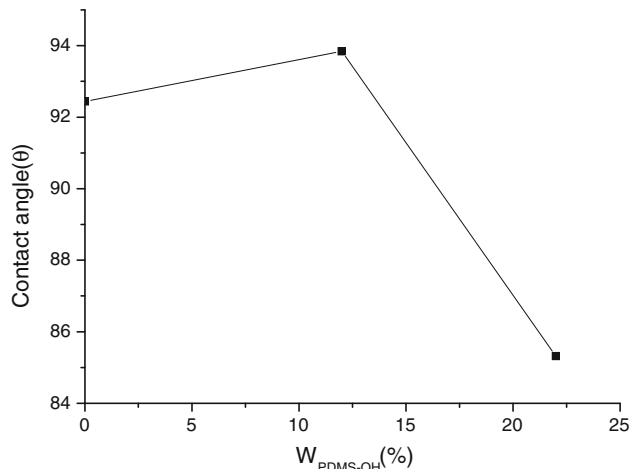


**Fig. 11** The values of contact angle for various concentration of PDMS-OH

pH is close to 7 after exposure for 8 h and remains approximately constant. The trend of concentration of calcium ions in solution is accord with that of pH, which is shown in Figs. 13 and 14. It is noticeable in the graph (Figs. 13, 14) that the pH value and calcium ions concentration is higher for untreated sample than the treated samples at the same time. This leads us to believe that a certain level of “protection” is being achieved by hybrid sol and the protective efficiency of the silica coating is similar to the commercial product.

The vapor permeability through the untreated carbonate stones is 0.32 mg/(cm<sup>2</sup> d). When TEOS-12 %PDMS hybrid sol was applied to carbonate stons, the reduction of vapor permeability is 66 %. It is known that traditional TEOS-based consolidants reduce liquid water uptake values to some extent, still leaving open some porosity to the environment for the necessary stone breathing. On the other hand, as the vapor permeability remained practically the same as for traditional TEOS-DBTL formulations [13], it can be assumed that stone porosity is similarly maintained open, so stone breathability is not put under risk.

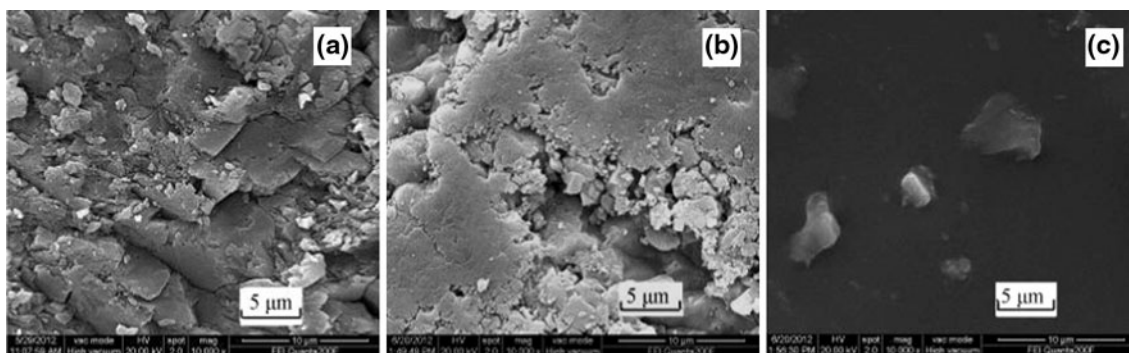


**Fig. 12** SEM image of limestone (a Untreated, b TEOS + 0.6 % *n*-octylamine, c TEOS + 0.6 % + *n*-octylamine + 12 % PDMS-OH)

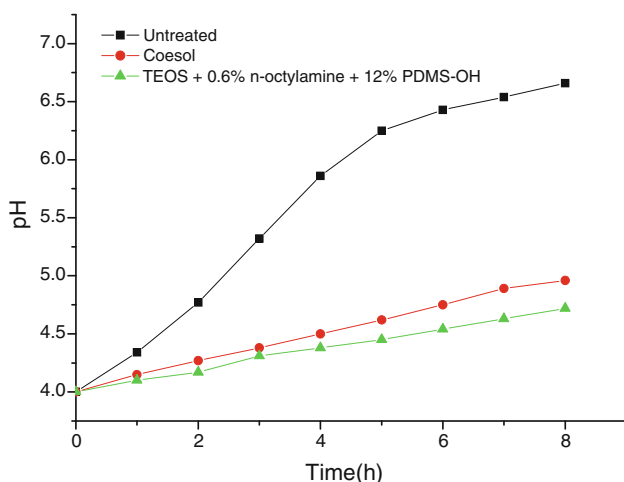


**Fig. 13** pH change of the solution with washing time

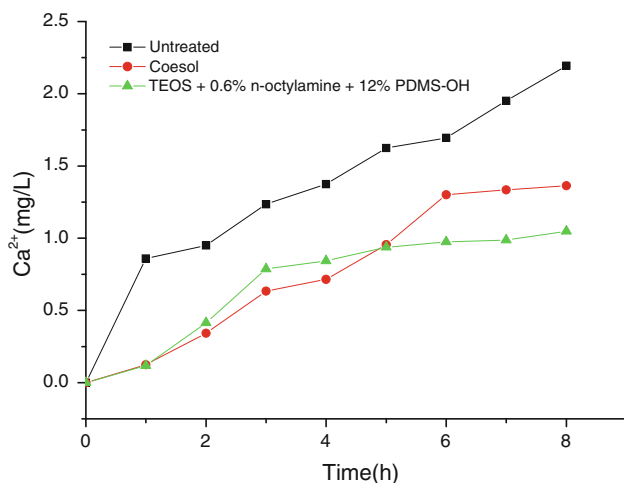


**Fig. 14** Ca<sup>2+</sup> change of the solution with washing time

#### 4 Conclusions

Film and monolithic xerogels were obtained by using a surfactant *n*-octylamine as a catalyst containing tetraethoxyorthosilicate (TEOS) and hydroxyl-terminated polydimethylsiloxane

as an additive. Volume shrinkage and density decrease with the addition of PDMS due to the significant increases in the dry materials “SiO<sub>2</sub>” contents with the addition of PDMS. TGA analysis shows ceramic yield decreases with the addition of PDMS and the presence of the PDMS in the hybrid xerogels results in a stronger thermal stability. With the addition of the PDMS, the pore size of silica becomes small, resulting in an increasing number of the interstitial holes with large size which are formed between silica particles. The contact angle of limestone treated with hybrid sol increased first and then decreased with the addition of PDMS. The protective performances were also evaluated by its ability to resist acid corrosion. The results reveals that the protective effects are satisfying.

**Acknowledgments** We are grateful to the Cultural Heritage Conservation Science and Technology of National Heritage Board and State Key Laboratory of Pollution Control and Resource Reuse open foundation for financial support under research projects 20110131, PCRRF11018.

#### References

1. Ngoic Lan TT, Nishimura R, Tsujino Y, Phuong T (2005) *Corros Sci* 47:1023
2. Xu F, Tang J, Gao S (2010) *J Cult Herit* 11:228
3. Poli T, Toniolo L, Chiantore O (2004) *Appl Phys A* 79:347
4. Rizzarelli P, La Rosa C, Torrisi A (2001) *J Cult Herit* 2:55
5. Ventolà L, Vendrell M, Giraldez P, Merino L (2011) *Constr Build Mater* 25:3313
6. Esposito Corcione C, Frigione M (2011) *Prog Org Coat* 72:522
7. He L, Liang J, Zhao X, Li W, Luo H (2010) *Prog Org Coat* 69: 352
8. Wheeler G (2005) *Alkoxysilanes and the consolidation of stone*. The Getty Conservation Institute, Los Angeles
9. Mosquera MJ, Pozo J, Esquivias L (2003) *J Sol Gel Sci Technol* 26:1227
10. Scherer GW (1990) *J Am Ceram Soc* 73:3
11. Mosquera MJ, De los Santos DM, Valdez-Castro L, Esquivias L (2008) *J Non-Cryst Solids* 354:645
12. Mosquera MJ, De los Santos DM, Rivas T (2010) *Langmuir* 26:6737
13. Zárraga R, Cervantes J, Salazar-Hernandez C, Wheeler G (2010) *J Cult Herit* 11:138

14. Xu F, Li D, Zhang H, Peng W (2012) *J Sol Gel Sci Technol* 61:429
15. Xu F, Li D, Zhang H, Chen W, Gao S (2010) *Chin J Chem* 28:1487
16. Allesandrini G, Aglietto M, Castelvetro V, Ciardelli F, Peruzzi R, Toniolo L (2000) *J Appl Polym Sci* 76:962
17. Salazar-Hernández C, Puy Alquizab MJ, Salgado P, Cervantes J (2010) *Appl Organometal Chem* 24:481
18. Illescas JF, Mosquera MJ (2011) *J Phys Chem C* 115:14624
19. Mosquera MJ, De los Santos DM, Rivas T (2010) *Langmuir* 26:6737
20. Fidalgo A, Ciriminna R, Iharco LM, Pagliaro M (2005) *Chem Mater* 17:6686
21. Illescas JF, Mosquera MJ (2011) *J Phys Chem C* 115:14624
22. Zhang X, Ye H, Xiao B, Yan L, Jiang B (2010) *J Phys Chem C* 114:19979
23. Tellez L, Rubio J, Rubio F, Morales E, Oteo JL (2003) *J. Mater Sci* 38:1773
24. Salazar-Hernández C, Zárraga R, Alonso S, Sugita S, Calixto S, Cervantes J (2009) *J Sol-Gel Sci Technol* 49:301